

# GEOMETRY AND DRAINAGE OF A RETREATING GLACIER OVERLYING AND RECHARGING A KARST AQUIFER, TSANFLEURON-SANETSCH, SWISS ALPS

## GEOMETRIJA IN ODTOK UMIKAJOČEGA SE LEDENIKA, KI PREKRIVA IN NAPAJA KRAŠKI VODONOSNIK, TSANFLEURON-SANETSCH, ŠVICARSKE ALPE

Vivian GREMAUD<sup>1</sup> & Nico GOLDSCHIEDER<sup>2</sup>

### Abstract

UDC 911.2:551.435.8:551.32

*Vivian Gremaud & Nico Goldscheider: Geometry and drainage of a retreating glacier overlying and recharging a karst aquifer, Tsanfleuron-Sanetsch, Swiss Alps*

Alpine glaciers store large amounts of freshwater contributing to groundwater recharge during warmer periods, but the interactions between glaciers and aquifers have rarely been investigated in detail. The Tsanfleuron-Sanetsch area, Switzerland, is an ideal test site to study glacier-aquifer interactions. It consists of a rapidly retreating glacier (2.8 km<sup>2</sup>) overlying a karst aquifer drained by a spring (mean discharge 600–700 L/s) used for drinking water supply and irrigation. The geometry and structure of the glacier were assessed by means of geophysical surveys, using radiomagnetotellurics (RMT). The estimated ice volume is 1.0 x 10<sup>8</sup> m<sup>3</sup> (0.92 x 10<sup>8</sup> m<sup>3</sup> water equivalent), but the glacier currently loses 1.5 m ice thickness per year. Field observations, flow measurements and tracer tests allowed characterisation of glacier drainage and aquifer recharge. Three recharge pathways have been identified: 1) The main glacial stream sinks into the aquifer via swallow holes 3 km downstream of the glacier mouth; 2) Numerous small meltwater streams sink underground shortly below the glacier front; 3) Subglacial meltwaters and supraglacial streams sink into the glacier via moulins and contribute to aquifer recharge through fractures and swallow holes underneath the glacier. Recharge and spring discharge display strong diurnal and seasonal variability, with a general high-flow period during snow and glacier melt from spring to autumn. Preliminary predictions of the future availability of spring water after disappearance of the glacier suggest that the discharge may decrease by 20–30%. Nearly all of this loss will occur in summer and autumn, presumably resulting in temporary water shortage.

**Keywords:** glacierised karst, groundwater recharge, ice thickness mapping, geophysics, radiomagnetotellurics, tracer test.

### Izvleček

UDK 911.2:551.435.8:551.32

*Vivian Gremaud & Nico Goldscheider: Geometrija in odtok umikajočega se ledenika, ki prekriva in napaja kraški vodonosnik, Tsanfleuron-Sanetsch, Švicarske Alpe*

Alpski ledeniki hranijo velike količine vode, ki v toplejšem delu leta prispevajo k zalagam podzemne vode, vendar je medsebojno vplivanje med ledeniki in vodonosniki le redko predmet podrobnih raziskav. Območje Tsanfleuron-Sanetsch v Švici je idealno za proučevanje vzajemnega vplivanja ledenikov na vodonosnike. Hitro umikajoč se ledenik (2,8 km<sup>2</sup>) prekriva kraški vodonosnik, ki napaja izvir s srednjimi pretočnimi vrednostmi med 600 in 700 l/s. Izvirsko vodo izrabljajo za pitno vodo in namakanje. Geometrija in struktura ledenika sta bili določeni s pomočjo geofizičnih raziskav, to je z uporabo radiomagnetotelurične metode (RMT). Izračunana prostornina ledenika je 10<sup>8</sup> m<sup>3</sup> (enakovredno 0,92 x 10<sup>8</sup> m<sup>3</sup> vode). Letno ledenik izgubi 1,5 m debeline. Terenska opazovanja, meritve toka in sledilni poskusi so omogočili proučevanje značilnosti odtekanja voda s talečega se ledenika ter napajanje vodonosnika. Ugotovljene so bile tri poti napajanja: 1) glavni ledeniški potok ponika v vodonosnik skozi ponore 3 km dolvodno pod ledeniški vrati, 2) številni manjši ledeniški potoki ponikajo neposredno pod čelom ledenika, 3) ledeniške vode ponikajo v ledenik skozi ledeniške razpoke in tečejo pod ledenikom ter napajajo vodonosnik skozi razpoke in ponore pod ledenikom. Napajanje in pretoki na izviru kažejo na izrazito vsakodnevno in sezonsko spremenljivost, z visokimi vrednostmi v času taljenja snega in ledu med pomladjo in jesenjo. Predhodne napovedi o razpoložljivosti izvirske vode po tem, ko bo ledenik izginil, domnevajo, da se bodo pretoki zmanjšali za 20-30%. Skoraj vsa ta izguba bo izrazita poleti in jeseni. Domnevno bo zaradi tega prihajalo do občasnega pomanjkanja vode.

**Ključne besede:** ledeniški kras, napajanje podzemne vode, kartiranje debeline ledenika, geofizika, radiomagnetotelurij, sledilni poskus.

<sup>1</sup> Centre of Hydrogeology (CHYN), University of Neuchâtel, 2009 Neuchâtel, Switzerland

<sup>2</sup> Technische Universität München (TUM), Department for Civil, Geo- and Environmental Engineering, Hydrogeology and Geothermics Group, Arcisstr. 21, 80333 Munich, Germany, E-mail: goldscheider@tum.de

Received/Prejeto: 5.11.2009

## INTRODUCTION

Since the maximum of the “Little Ice Age” in the middle of the 19<sup>th</sup> century, all alpine glaciers have lost much of their length and volume (e.g. Greene *et al.* 1999; Paul *et al.* 2004). Glacier retreat has already, and will continue to, influence the availability and temporal variability of hydraulically-connected freshwater resources, with implications for ecosystems (Cannone *et al.* 2008), drinking water supply, agriculture and hydropower (Loukas *et al.* 2002; Viviroli & Weingartner 2004). Glaciers store water as snow and ice during cold periods and release it during warm periods (Benn & Evans 2010). During times of glacial retreat, increased meltwater production can lead to temporarily higher freshwater availability in connected streams and aquifers. However, from a long-term perspective, a loss of glaciers as intermediate storage reservoirs is expected to result in local or temporary water shortages, particularly during long dry summers (Schaeffli *et al.* 2007; Seidel *et al.* 1998).

To date, glaciology and hydrogeology are separate disciplines; only a few studies investigate glacier-aquifer relations, e.g. numerical simulations of large-scale groundwater flow beneath ice shields (Flowers *et al.* 2003). Published studies evaluating climate change im-

pacts on glacier-aquifer dynamics on a catchment scale are scarce. The relations between glaciers and karst aquifers have previously been studied in the Rocky Mountains of Alberta, Canada (Smart 1983, 1996, 1997; Smart & Ford 1986).

In the Tsanfleuron-Sanetsch area in the Swiss Alps, a regional karst aquifer is drained by a spring (Glarey) at its lowest point and overlain by a rapidly retreating glacier in its upper part (Figs. 1 and 2). The spring is used for drinking water supply of a community (Conthey) and for irrigation. This test site is thus ideal for studying glacier-aquifer interrelations and for evaluating possible impacts of glacier retreat on connected freshwater resources. Glaciologists have studied the Tsanfleuron glacier, focusing on its temperature distribution, rheology, and ice-flow dynamics (Chandler *et al.* 2008; Hubbard 2002; Hubbard *et al.* 2000; Sharp *et al.* 1989). Recently, hydrogeologic research has revealed the relations between the geological structure and the drainage pattern in the karst aquifer (Gremaud *et al.* 2009).

The present study combines glaciological and hydrogeologic methods; it focuses on the role of the glacier as an intermediate freshwater storage reservoir recharging

the aquifer and ultimately contributing to drinking water supply. The objectives of this study are:

1. Determine the geometry of the glacier, i.e. its surface area and average thickness, so as to determine the ice volume and the equivalent freshwater quantity;

2. Obtain information on the structure and morphology of the glacier-limestone interface, i.e. the hidden karst landscape below the glacier.

3. Investigate, characterize and classify recharge processes by which meltwaters enter the aquifer underneath the glacier and beyond its front.

The goals were obtained by a combination of geophysical and hydrogeologic methods, such as radiomagnetotellurics (RMT) to determine ice thickness, and tracer tests

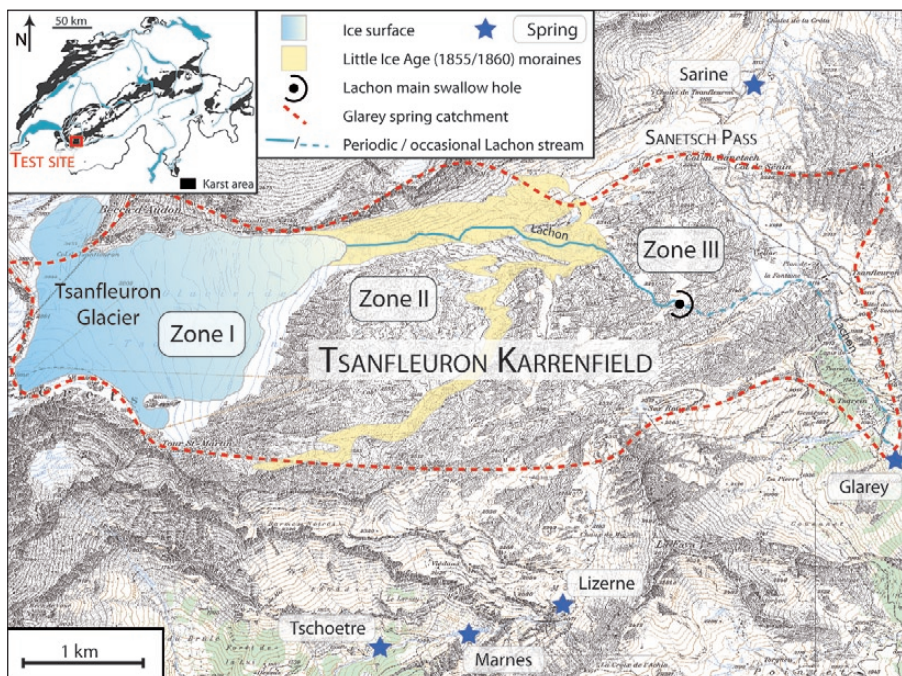


Fig. 1: Location and overview of the Tsanfleuron-Sanetsch glacier and karst system (Swiss Alps), which is subdivided into three zones: I. glacier on top of karst aquifer; II. limestone between current glacier front and end moraine from 1855/60; III. limestone exposed since the end of the Würm Ice Age. The main glacier stream (Lachon) typically sinks into swallow holes in zone III; only during extreme high-flow conditions, it continues beyond this point. Copyright for topographic maps used in this article: Swisstopo 2006.

to characterise recharge processes. The study is part of a larger project with the ultimate goal of obtaining prognoses on the future availability and variability of alpine

freshwater resources under conditions of continued glacial retreat and eventual disappearance of small glaciers.

## GEOLOGIC AND HYDROGEOLOGIC SETTING

### GEOLOGIC FRAMEWORK

The study area belongs to the Helvetic zone of the Alps, a SW-NE striking zone of tectonic nappes mostly consisting of alternating Jurassic to Paleogene limestone, marl and sandstone. The Tsanfleuron glacier overlies Cretaceous limestone (Barremian-Aptian) that outcrops on large parts of the land surface (Fig. 2). The thick-bedded to massive limestone is 100–120 m thick in the study area. This formation, referred to as *Urgonian* or *Schrattenkalk*, is one of the most important karstifiable geologic units in the Alps, due to its mechanical strength and mineralogi-

strata are folded, with SW-NE trending fold axes (Steck *et al.* 2001). The entire zone from the Tsanfleuron glacier to the Sanetsch pass is formed by a large, wide anticline plunging towards the NE at an angle of about 10° (Fig. 3). The southward-bordering, narrow, overturned syncline forms the limit of the karst system. Prominent fracture directions are ENE, E and SE.

### KARST AQUIFER

Gremaud *et al.* (2009) have studied the hydrogeology of this karst system by means of multi-tracer tests with a total of 19 injections, along with geologic, hydrologic and speleological observations, and found that the Urgonian and Eocene limestones constitute one hydraulically-connected aquifer. Five springs along the southern to northeastern borders of the area drain the system (Fig. 1). The major part of the karst surface and glacier is drained by the Glarey spring in the SE (consisting of the main spring and a nearby intermittent overflow), with a discharge ranging from 34 L/s in winter to 4800 L/s during snowmelt and storm rainfall, with a mean discharge of 667 L/s (2004–2009). Underground flow toward this spring occurs parallel to the stratification, near the base of the aquifer, on top of the underlying marl. Therefore, the flow follows the dip of



Fig. 4: Fig. 2: Impression of the Tsanfleuron glacier overlying the Urgonian karst aquifer. Rock surfaces are polished and show striations and hummocks. Glacial meltwater streams flow over limestone, typically for several tens of metres, but eventually sink underground via fractures or shafts (Photo: N. Goldscheider, autumn 2009).

cal purity (97% calcite; Goldscheider 2005). Locally, it is overlain by thinly-bedded Eocene nummulitic limestone and other rock types. The formation below the Urgonian limestone consists mainly of marl, about 100 m thick. The

the strata, from the crest of the wide anticline, down its SE limb toward the narrow syncline, which collects all groundwater and conducts it to the spring, located at the lowest point where this syncline is exposed, at

1,550 m asl (Fig. 3). A similar drainage pattern with a high degree of “statigraphic flow control” has also been described for other Helvetic karst systems (Goldschieder 2005).

Dominant transit times towards Glarey spring are in a range of 5–57 h (obtained from peak times of tracer breakthrough curves) with recoveries of 5–80%. Only

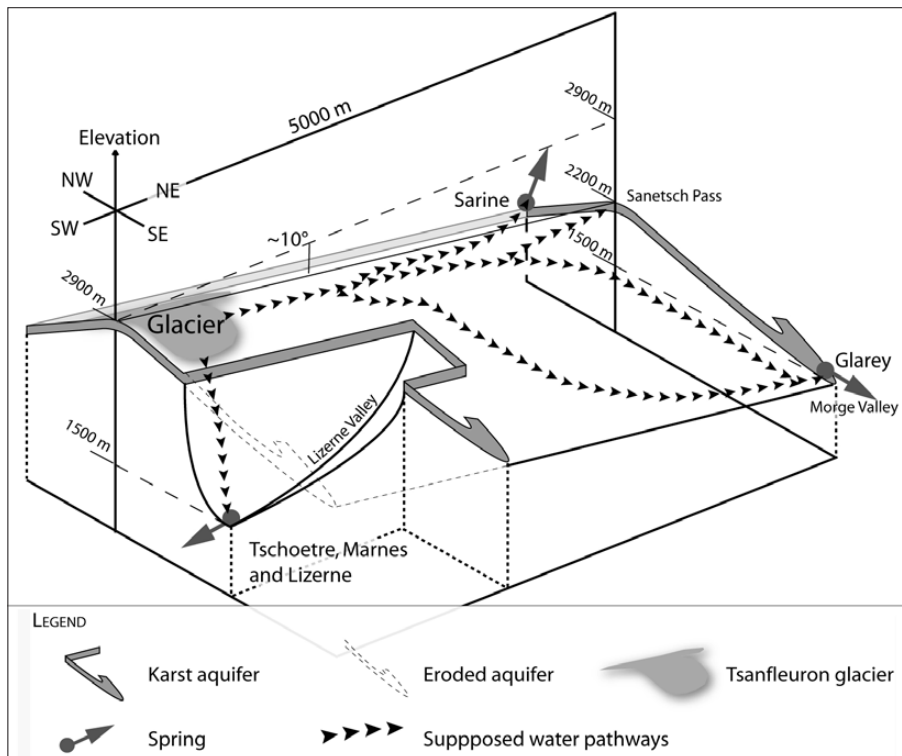


Fig. 3: Schematic fence diagram illustrating the geologic structure and drainage of the Tsanfleuron-Sanetsch glacier-karst system. The Urganian-Eocene karst aquifer is highlighted in grey. Arrows indicate inferred schematic flow paths toward three groups of springs: Glarey spring drains most of the area; the other springs drain marginal parts. Connections have been established by 19 tracer tests, but precise pathways are not known.

marginal parts of the karrenfield are drained by the other springs in the S and NE. The three karst springs in the S discharge from Upper Jurassic limestone, but tracer tests demonstrated rapid connection between glacial meltwaters sinking into the Cretaceous-Eocene aquifer and these springs (Fig. 3). The water consequently crosses the entire stratigraphic sequence, including several marl aquicludes, probably along deep open fractures, with transit times of 15–32 h. The Sarine spring drains a small strip of karst limestone in the NE part of the area.

#### ZONES OF SURFACE KARST DEVELOPMENT

There are three zones of karst development (Gremaud *et al.* 2009): (I) underneath the glacier, (II) between the

glacier front and the end moraine from 1855/1860 (“Little Ice Age”) and (III) below this moraine (Fig. 1). The limestone surface underneath the glacier cannot be directly observed, but as the glacier is rapidly retreating (300 m between 2000 and 2008; VAW 2009), observations near the glacier front provide insights into subglacial geomorphology and hydrology. In this zone, rock surfaces are polished and the epikarst has been removed by glacial erosion or has never formed.

The basal ice includes plucked material that creates striations on limestone surfaces (Fig. 2). In zone II, this rock debris forms a thin, discontinuous ablation till. Carbonate precipitates occur on lee sides of subglacial bedrock hummocks, now exposed below the current glacier front (Hubbard & Hubbard 1998). Nye channels cut into the rock surface by meltwater indicate that at least parts of the subglacial drainage occur along the ice-rock interface (Bates *et al.* 2003; Grust 2004). After glacier retreat, meltwater streams often flow several tens of metres in these channels or over polished limestone surfaces before sinking into shafts or fractures. Such swallow holes are present everywhere in the area. During spring and early summer snowmelt, the zone of active swallow holes is extensive; but in dry summer and autumn periods, active swallow holes can only be found near the glacier front. Rainfall activates swallow holes across zone II.

In many alpine areas, the combined action of mechanical erosion by glaciers and flowing waters has formed the landscape; in karst areas, most water drains underground, so that the result of pure glacial erosion can be observed. Zone II of the study area includes large depressions, hundreds of metres wide and tens of metres deep. Some of them are bordered by steep walls, caused by plucking of fracture-bounded limestone blocks by the flowing glacier. Similar geomorphologic and hydrologic phenomena have been observed in a glacierised karst region of the Canadian Rocky Mountains (Ford 1983).

In zone III, the landscape has been exposed to karstification since the end of the Würm Ice Age, about 10,000 years ago. Karrenfields are partly covered by thin soil and alpine vegetation; The name Tsanfleuron comes from the French *champ fleuri*, which means flower meadow. Due to a well-developed epikarst, diffuse infiltration pre-

dominates, with two exceptions: The main glacier stream (Lachon), which first flows over moraine, sinks into several swallow holes in the centre of zone III (Fig. 1). At the eastern margin of the area, several allogenic streams sink underground near the marl-limestone contact.

## METHODS

### GEOPHYSICAL MEASUREMENT OF GLACIER THICKNESS

Glacier thickness was measured by the radiomagnetotelluric (RMT) method. Georadar and seismics are often used for glacier surveys: Seismics allows for greater investigation depth; georadar is efficient for imaging shallow glacier structures (Senechal *et al.* 2003). RMT was selected for his study because the equipment is portable, and the method delivers robust information on layer thickness (provided resistivity contrasts are sufficiently high). RMT uses electromagnetic waves emitted at remote stations at frequencies of 12–240 kHz. The method delivers values of apparent resistivity ( $\rho_a$ ) and phase lag (between electric and magnetic fields) that can be inverted to produce a model of true resistivity versus depth below each measurement point (vertical sounding). The higher the frequency, the better the resolution but the shallower the investigation depth (Bechtel *et al.* 2007):

$$d = 503 \sqrt{\frac{\rho}{f}} \quad (1)$$

Where  $d$  is investigation depth or skin depth (m),  $\rho$  is resistivity ( $\Omega\text{m}$ ) and  $f$  is frequency (Hz). Four frequencies were used, 234, 183, 77.5 and 19.6 kHz. As ice resistivity critically depends on meltwater saturation and consequently varies with temperature, the investigation depth is also variable (Kulesa 2007). A two-layer model was used for the data inversion: glacier ice overlying limestone, where ice thickness ( $Z$ ), ice resistivity ( $\rho_1$ ), and limestone resistivity ( $\rho_2$ ) are the three fit parameters (Fig. 4). Variable ice resistivity poses no problem, as it is always significantly lower than limestone resistivity, i.e. the contrast is sufficiently high.

During two glacier surveys in the summers of 2007 and 2008, RMT measurements were done at 226 points, located by means of GPS with a precision of 2 m horizontally and 3 m vertically. The mean distance between measurement points is 90 m, but the distribu-

tion is heterogeneous, because of crevasses and other terrain difficulties. Ten points were measured in both years, during different times of the day, and delivered reproducible results with a mean error of 3.8 m. Two software tools were used for data inversion: FITVLF2 and Gmin (developed by J. Thierrin, 1988, and P.A. Schnegg, 2002, respectively, University of Neuchâtel, unpublished). When the two codes delivered inconsis-

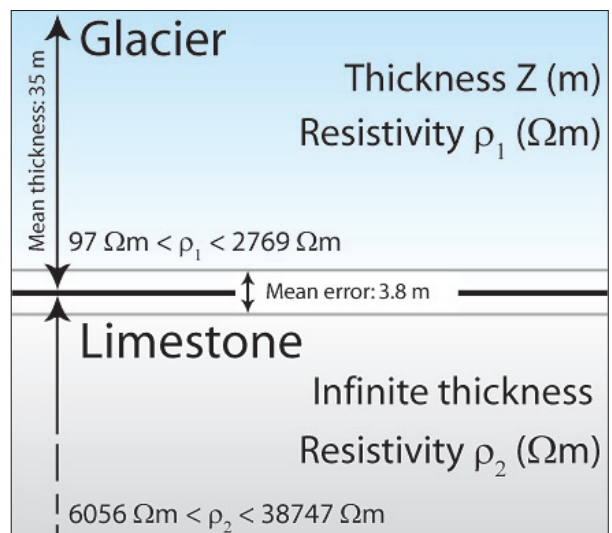


Fig. 4: Illustration of the two-layer model used for the RMT ice-thickness mapping. The fit parameters include ice thickness, ice resistivity, and limestone resistivity. Ranges of obtained resistivity values are indicated. Ice resistivity varies as a function of water saturation, but the resistivity contrast is always sufficiently high to obtain clear results, confirmed by repeated measurements at 10 selected points in 2007 and 2008, which delivered reproducible results (mean error 3.8 m).

tent results, the respective data point was eliminated. Interpolation (kriging) of the measured ice thickness at all 187 valid measurement points yielded a map of ice thickness in 2007/2008. Due to rapid glacier retreat, such maps are only snapshots.

Tab. 1: Summary of the tracer injections and flow rates of the meltwater streams sinking into moulin used for tracer injections at Tsanfleuron glacier in September 2008; locations of injection sites see in Fig. 6.

	Uranine (U)	SulfoG (SG)	Naphthionate (N)
Elevation Z	2850 m	2738 m	2700 m
Tracer quantity	200 g	400 g	1000 g
Estimated flow rate	5 L/s	15L/s	100 L/s



Fig. 5: Tracer injections at Tsanfleuron glacier: (A) Uranine, (B) Sulforhodamine G, (C) Naphthionate (Photos: V. Gremaud).

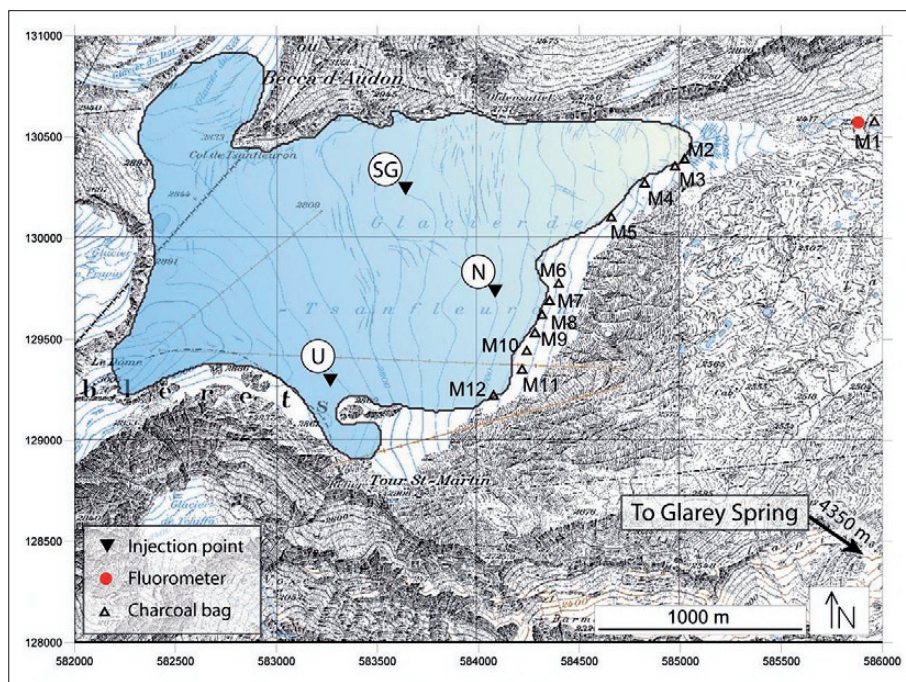


Fig. 6: Location of the injection points for Uranine (U), Sulforhodamine G (SG) and Naphthionate (N), and the monitoring sites (M1–M12). The Glarey spring (outside the map) is the principal drainage point of the groundwater system and was also monitored.

### MULTI-TRACER TEST TO CHARACTERISE GLACIER-AQUIFER RELATIONS

Three tracer injections were done at Tsanfleuron glacier on 11 September 2008. The fluorescent dyes Uranine, Sulforhodamine G (SulfoG) and Naphthionate were used

as tracers. The three injection sites represent different recharge pathways (Tab. 1, Figs. 5 and 6): Uranine was injected at the top of the glacier, near its southern edge, into a moulin with an estimated flow rate of 5 L/s. SulfoG was injected into a stream (15 L/s) sinking into a crevasse that drains a shallow depression in the northern part of the glacier, 1.4 km west of the glacier terminus. Naphthionate was injected near the central part of the glacier front into a large meltwater stream (100 L/s) sinking into a deep moulin.

For monitoring, a field fluorometer (GGUN-FL30, Neuchâtel, Switzerland) was installed into the main glacier stream (Lachon), 860 m downstream of the glacier mouth (M1, Fig. 6); charcoal bags were put in 12 meltwater streams, including M1 (for comparison between fluorometer and charcoal results), two tributaries of the main stream (M2, M3) and 9 streams emerging at the glacier front and sinking into the karst aquifer via swallow holes (M4–M12, Fig. 6). Charcoal bags were selected for monitoring because of the large number and remoteness of sites. Usually, charcoal bags are not recommended for Naphthionate detection because of interference with organic carbon (Goldscheider *et al.* 2008), but glacial meltwaters contain very little organic carbon and the expected tracer concentrations were high. Glarey spring was monitored using an auto-sampler (6712C, ISCO, Lincoln, USA) and a field fluorometer. All samples were analysed in the CHYN laboratory (Neuchâtel) with a spectrofluorometer (Perkin Elmer LS50B).

contain very little organic carbon and the expected tracer concentrations were high. Glarey spring was monitored using an auto-sampler (6712C, ISCO, Lincoln, USA) and a field fluorometer. All samples were analysed in the CHYN laboratory (Neuchâtel) with a spectrofluorometer (Perkin Elmer LS50B).

## RESULTS AND DISCUSSION

## GLACIER THICKNESS, SUBGLACIAL KARST MORPHOLOGY, GLACIAL FRESHWATER STORAGE

Fig. 7 presents the ice thickness map of Tsanfleuron glacier in summers 2007/2008, based on 187 valid RMT measurements and a glacier borehole at the SW corner of the area (there is no RMT measurement point near

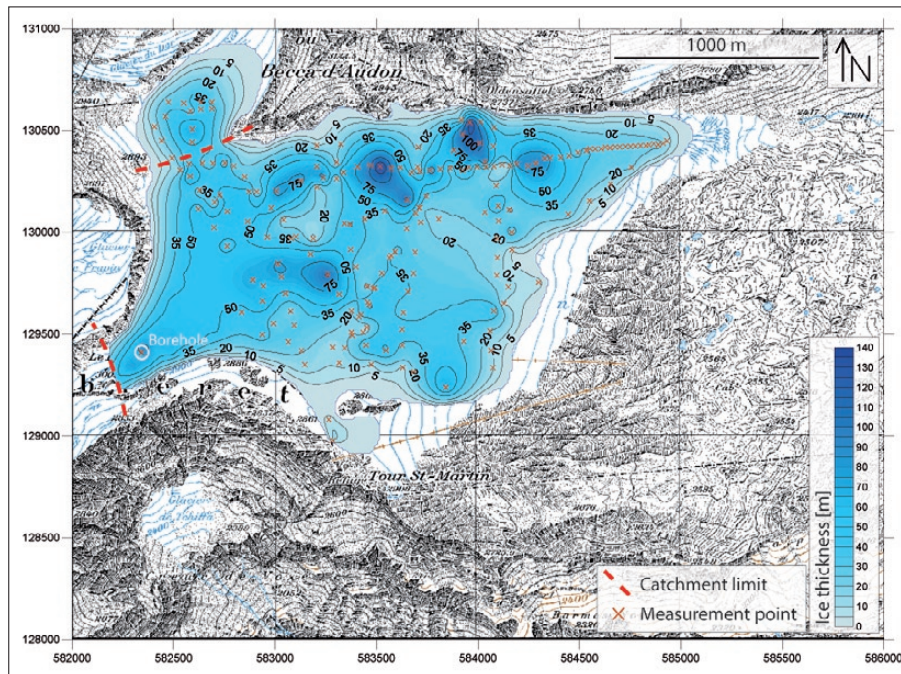


Fig. 7: Ice thickness map of Tsanfleuron glacier in 2007/2008, based on 187 valid RMT soundings and a glacier borehole. The NW zone of the glacier is probably not within the catchment of the Glarey spring (based on bedrock geology and topography) and was not included in the estimations of ice volume. The thick northern part forms a glacier tongue; the southern sector is a thin ice layer overlying limestone. The heterogeneous pattern of ice thickness reflects the uneven rock surface relief below the glacier.

this borehole that would allow comparison; we learned of this borehole only recently, after completion of the field surveys). As the reproducibility of the results has been confirmed by repeated measurements in two subsequent years (described above and illustrated in Fig. 4), the map is sufficiently precise to estimate the ice volume and characterise the geometry of the glacier and subglacial morphology. The mean ice thickness is 35 m, with a maximum of 138 m near the northern margin of the glacier and only 15 near its centre. Based on this map and field observations, the glacier can be subdivided into two parts: a thick northern part, which fills a W-E trending valley and forms a glacier tongue in its lowest part; and a central and southern zone consisting of a thin layer of

ice overlying a shelf of Urgonian limestone (Fig. 2). The subglacial bedrock topography contains depressions and knobs, especially in the northern part, where the geology is heterogeneous and also includes softer rocks, resulting in differential glacial erosion. The southern sector also shows several wider oscillations; The subglacial morphology (zone I) consequently resembles the karst landscape in the glacier forefield (zone II).

Based on the glacier thickness map (and considering measurement accuracy and uncertainties resulting from interpolation and system boundaries), the ice volume within the catchment of the Glarey spring (as indicated in Fig. 7) is estimated at  $1.0 \times 10^8 \text{ m}^3$  ( $\pm 10\%$ ), corresponding to  $0.92 \times 10^8 \text{ m}^3$  ( $\pm 10\%$ ) freshwater available for recharge, assuming an ice-water density ratio of 0.92 (Benn & Evans 2010). Data from the Swiss Glacier Monitoring Network (VAW 2009) and field observations indicate that the glacier currently loses about 15 m in length and 1.5 m in thickness per year. In 2008, the glacier occupied  $2.8 \text{ km}^2$ , so the estimated annual ice loss would be  $4.2 \times 10^6 \text{ m}^3$  ( $3.9 \times 10^6 \text{ m}^3$  of freshwater). Sublimation and evaporation losses from glaciers are small compared to meltwater production (Benn & Evans 2010). Therefore, most of this volume is presumed to contribute to aquifer recharge (if sufficient aquifer storage is available, which is the case here). This quantity represents a transient surplus of water that is available during periods of glacier retreat but will be missing when the glacier has disappeared. The annual water volume discharged at Glarey spring is  $2.1 \times 10^7 \text{ m}^3$ , so the projected missing water volume corresponds to ca. 20% of the spring flow.

## TRACER TEST RESULTS AND GLACIER-AQUIFER-SPRING DRAINAGE PATHWAYS

The tracer injections delivered positive results and gave insights into the relations between the glacier, the aquifer,

and the spring. Results obtained from charcoal bags installed at 12 meltwater streams around the glacier (M1–M12, Fig. 6) are summarised in Tab. 2. SulfoG was found in monitoring sites M1 and M3, contributing to the main glacier stream (Lachon). Naphthionate was detected at very high levels at M6, M10 and M11, demonstrating connection between the supraglacial meltwater stream sinking into the moulin (N in Fig. 6) and three subglacial meltwater streams emerging at the glacier front and sink-

and the spring, presumably via subglacial swallow holes. The two distinct peaks of the Uranine BTC may point to the presence of two subglacial swallow holes connected to different karst conduits (Fig. 8 A). However, high diurnal meltwater discharge variations can also create multi-peak BTCs (Gremaud *et al.* 2009).

SulfoG recovery is higher at Glarey spring (14.1%) than in the Lachon stream (2.5%), while transit times are similar, although the distance to the spring is 2.6 times

Tab. 2: Results of charcoal bags installed at monitoring sites M1–M12 (location see Fig. 6). Legend: Napht. = Naphthionate; + means positive results, / means tracer not detected.

	M1	M2	M3	M4	M5	M6	M7	M8	M9	M10	M11	M12
Altitude (m)	2380	2519	2537	2570	2607	2636	2646	2644	2645	2648	2649	2674
Uranine	/	/	/	/	/	/	/	/	/	/	/	/
SulfoG	+	/	+	/	/	/	/	/	/	/	/	/
Napht.	/	/	/	/	/	+	/	/	/	+	/	+

Tab. 3: Summary of tracer test results at the main glacier stream (Lachon) and the Glarey spring. Cmax/M means maximum concentration normalised by injected tracer mass.

	<i>Lachon stream</i>		<i>Glarey spring</i>	
	SulfoG	Uranine	SulfoG	Naphthionate
Distance (m)	2,460	6,570	6,325	5,785
Peak transit time (h)	17.9	19.5	19.6	15.3
Recovery (%)	2.5	40.7	14.1	32.7
Cmax/M (1/m <sup>3</sup> )	1.1 × 10 <sup>-4</sup>	2.3 × 10 <sup>-5</sup>	1.2 × 10 <sup>-5</sup>	6 × 10 <sup>-6</sup>

ing into three swallow holes several tens of metres downhill. Uranine was not detected in any of the 12 monitoring sites around the glacier, suggesting that all meltwaters sinking into this moulin (U in Fig. 6) infiltrate into the underlying karst aquifer via subglacial swallow holes.

The fluorometer installed in the Lachon stream (M1, Fig. 6) recorded a SulfoG breakthrough curve (BTC; Fig. 8), while the other two tracers were not detected. This is consistent with the hypothesis that only the northern zone of the glacier, which forms a glacier tongue, drains toward the principal glacier stream, while the central and southern part are drained by the immediately underlying karst aquifer. The irregular shape of the BTC can be explained by the highly variable flow rate of this meltwater stream. The peak time is 17.9 h and the recovery is only 2.5%, suggesting that large parts of the tracer went elsewhere (Tab. 3).

All three tracers were detected at the Glarey spring (Tab. 3), where a fluorometer and auto-sampler were installed, confirming that this spring is the main drainage point of the entire Tsanfleuron-Sanetsch glacier and karst system. Uranine was only detected at this spring but not at any monitoring site around the glacier, confirming direct and rapid connection between the glacier moulin

larger than to the monitoring site in the stream (Tab. 3 and Fig. 8 B and C). These findings demonstrate that there are two recharge pathways between the northern part of the glacier and the spring: 1) infiltration into subglacial swallow holes and direct underground passage in the karst aquifer toward the spring (19.6 h for 6,325 m), and 2) drainage near the glacier base towards the main glacier stream (17.9 h for 2,460 m), which sinks underground via swallow holes 3 km farther downstream; these swallow holes are connected to the spring, as demonstrated by previous tracer tests (6.1 h for 2,274 m, Gremaud *et al.* 2009). The second peak of the SulfoG BTC (Fig. 8 C) can be interpreted as the arrival of tracer that travelled along this second pathway.

Naphthionate was detected in three charcoal bags installed at the glacier front and also arrived at the Glarey spring, which allows identification of the relevant pathways: The supraglacial meltwater stream sinking into the glacier moulin (N in Fig. 6) flows at the glacier-limestone interface along three different Nye channels, reappears at the glacier front and then sinks underground into three swallow holes, which are connected to the spring. The Naphthionate BTC (obtained from laboratory analyses of water samples, which are more reliable for



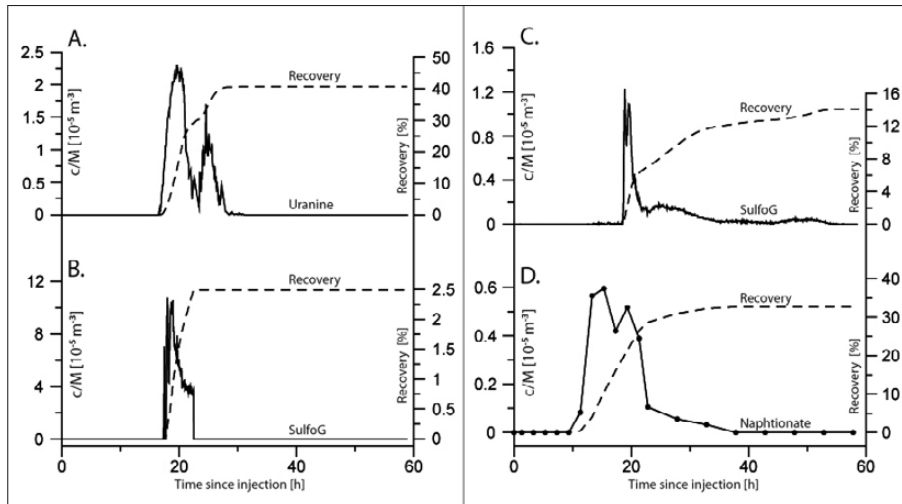


Fig. 8: Breakthrough curves and tracer recoveries obtained by the three injections at Tsanfleuron glacier. To enable comparison, normalised concentrations are shown, i.e. concentrations divided by injection mass ( $c/M$ ). (A) Uranine at Glarey spring, (B) SulfoG in the main glacier stream (Lachon), (C) SulfoG and (D) Naphthionate at Glarey spring. The abrupt decrease of SulfoG in the Lachon stream is not an artefact but presumably the result of a meltwater wave flushing all tracer previously stored in stagnant zones of the streambed.

this dye than measurements with field fluorometers) displays two peaks, which may correspond to different Nye channels and swallow holes (Fig. 8 D).

## CONCLUSIONS AND OUTLOOK

The combined use of geophysical and hydrogeologic methods made it possible to assess the geometry and volume of the Tsanfleuron glacier, estimate the stored freshwater volume, characterise hydrologic glacier-aquifer relations, and make preliminary prognoses concerning the future availability of freshwater from the Glarey spring, which is used for drinking water supply and irrigation. The glacier can be subdivided into a northern zone forming a glacier tongue, and a thin, “pancake-like” central to southern zone. The subglacial morphology includes depressions and mounts, similar to the karst landscape below the recent glacier front that has been exposed due to rapid glacier retreat since 1855/1860. The northern zone of the glacier partly drains via subglacial swallow holes and partly contributes to the main glacier stream that sinks underground 3 km downstream of the glacier mouth (Fig. 9 A). The central and southern part drains via numerous swallow holes underneath the glacier and near its front (Fig. 9 B). Similar drainage patterns have been described for glacierised karst systems in the Rocky Mountains, Canada (Smart 1983, 1997).

In 2007/2008, Tsanfleuron glacier includes about 100 Mm<sup>3</sup> of ice (92 Mm<sup>3</sup> water equivalent). Glaciers accumulate snow and ice in winter and release meltwater

in summer. Under equilibrium conditions (no retreat or advancement), glaciers do not exert much influence on the long-term water budget of a hydrologic basin, as there is balance between accumulation and ablation by sublimation, evaporation and meltwater production, the latter contributing to runoff and recharge. Glaciers at equilibrium mainly influence the variability of connected freshwater resources by delivering meltwater during warm periods. However, retreating glaciers do alter the water balance: The Tsanfleuron glacier currently loses 1.5 m thickness per year, corresponding to  $3.9 \times 10^6$  m<sup>3</sup> of water. This is a transient quantity that is available today but will be missing when the glacier disappears. Although reliable prognoses concerning climate change and glacier retreat are problematic, simple extrapolation of the current trend suggests that this small glacier might have disappeared by 2035. This will reduce the present-day annual discharge of the Glarey spring ( $2.1 \times 10^7$  m<sup>3</sup>) by ca. 20%. Preliminary water balance estimations (that need to be refined and will be presented in detail in a follow-up paper) even suggest a possible loss of 30%. Nearly all of this spring flow loss of 20–30% would occur during summer and autumn, causing temporary water shortage.

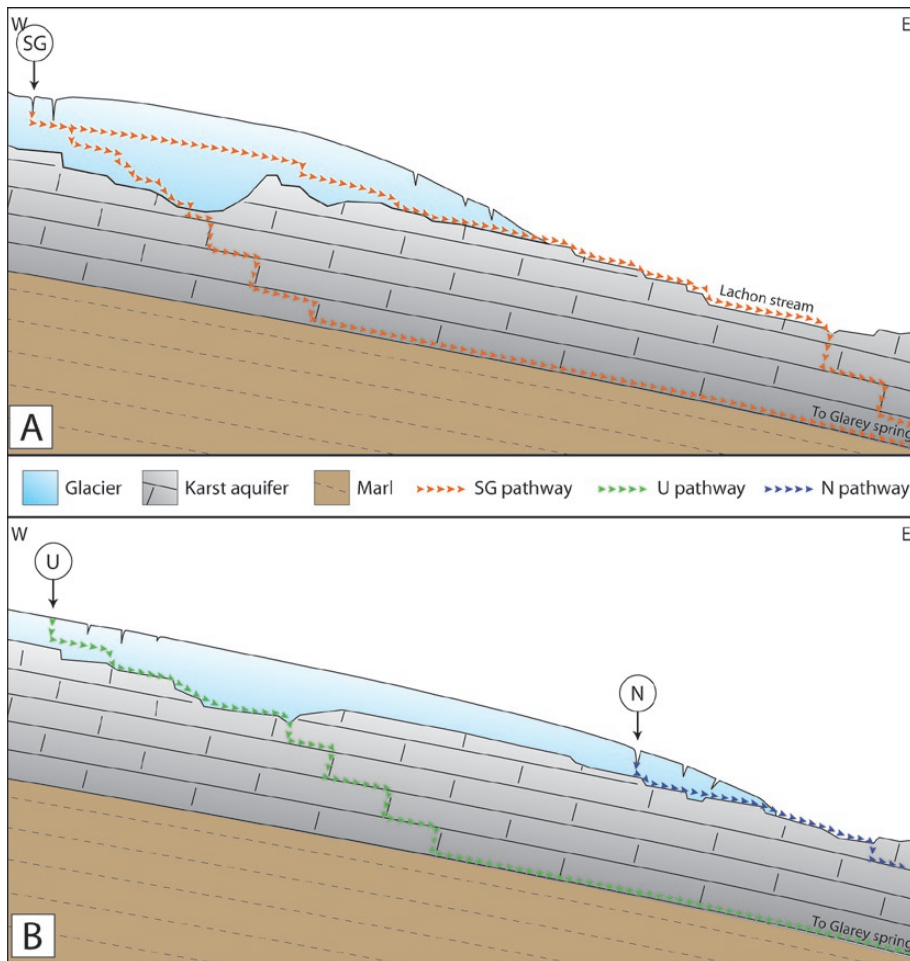


Fig. 9: Schematic illustration of glacier-aquifer relations (A) in the northern zone, and (B) in the central to southern zone of Tsanfleuron glacier, based on geophysical glacier surveys and tracer tests with Sulforhodamine G (SG), Uranine (U) and Naphthionate (N).

### ACKNOWLEDGEMENT

The GLACIKARST project is funded by the Swiss National Science Foundation (grant n° 200020-121726/1). We thank Sébastien Deyres, Mathieu Beck, Karin Spiegelhalter and Roberto Costa for help during field work,

Pierre-André Schnegg for measurement instruments, Lars Theiler for glacier borehole data, and Timothy Bechtel, Christopher Smart and an anonymous reviewer for helpful comments.

### REFERENCES

Bates, P.D., Siegert, M.J., Lee, V., Hubbard, B.P. & P.W. Nienow, 2003: Numerical simulation of three-dimensional velocity fields in pressurized and nonpressurized Nye channels.- *Annals of Glaciology*, 37, 281–285.

Bechtel, T.D., Bosch, F.P. & M. Gurk, 2007: Geophysical methods.- In: N. Goldscheider & D. Drew (Eds.), *Methods in karst hydrogeology*. International Contributions to Hydrogeology, Taylor & Francis, pp. 171–199, London.

- Benn, D.I. & D.J.A. Evans, 2010: *Glaciers and Glaciation*.- Hodder Arnold Publication, pp. 816, London.
- Cannone, N., Diolaiuti, G., Guglielmin, M. & C. Smiraglia, 2008: Accelerating climate change impacts on alpine glacier forefield ecosystems in the European Alps.- *Ecological Applications*, 18, 3, 637–648.
- Chandler, D., Hubbard, B., Hubbard, A., Murray, T. & D. Rippin, 2008: Optimising ice flow law parameters using borehole deformation measurements and numerical modelling.- *Geophysical Research Letters*, 35, 12, article number L12502.
- Flowers, G.E., Bjornsson, H. & F. Palsson, 2003: New insights into the subglacial and periglacial hydrology of Vatnajökull, Iceland, from a distributed physical model.- *Journal of Glaciology*, 49, 165, 257–270.
- Ford, D.C., 1983: The physiography of the Castleguard karst and Columbia icefields area, Alberta, Canada.- *Arctic and Alpine Research*, 15, 4, 427–436.
- Goldscheider, N., 2005: Fold structure and underground drainage pattern in the alpine karst system Hochifen-Gottesacker.- *Eclogae Geologicae Helvetiae*, 98, 1, 1–17.
- Goldscheider, N., Meiman, J., Pronk, M. & C. Smart, 2008: Tracer tests in karst hydrogeology and speleology.- *International Journal of Speleology*, 37, 1, 27–40.
- Greene, A.M., Broecker, W.S. & D. Rind, 1999: Swiss glacier recession since the Little Ice Age: Reconciliation with climate records.- *Geophysical Research Letters*, 26, 13, 1909–1912.
- Gremaud, V., Goldscheider, N., Savoy, L., Favre, G. & H. Masson, 2009: Geological structure, recharge processes and underground drainage of a glacierised karst aquifer system, Tsanfleuron-Sanetsch, Swiss Alps.- *Hydrogeology Journal*, 17, 8, 1833–1848.
- Grust, K., 2004: *The hydrology and dynamics of a glacier overlying a linked-cavity drainage system*.- PhD thesis, Dpt. of Geography and Geomatics, University of Glasgow, pp. 210.
- Hubbard, B., 2002: Direct measurement of basal motion at a hard-bedded, temperate glacier: Glacier de Tsanfleuron, Switzerland.- *Journal of Glaciology*, 48, 160, 1–8.
- Hubbard, B. & A. Hubbard, 1998: Bedrock surface roughness and the distribution of subglacially precipitated carbonate deposits: Implications for formation at Glacier de Tsanfleuron, Switzerland.- *Earth Surface Processes and Landforms*, 23, 3, 261–270.
- Hubbard, B., Tison, J.L., Janssens, L. & B. Spiro, 2000: Ice-core evidence of the thickness and character of clear-facies basal ice: Glacier de Tsanfleuron, Switzerland.- *Journal of Glaciology*, 46, 152, 140–150.
- Kulesa, B., 2007: A Critical Review of the Low-frequency Electrical Properties of Ice Sheets and Glaciers.- *Journal of Environmental & Engineering Geophysics*, 12, 3, 23–36.
- Loukas, A., Vasiliades, L. & N.R. Dalezios, 2002: Climatic impacts on the runoff generation processes in British Columbia, Canada.- *Hydrology and Earth System Sciences*, 6, 2, 211–227.
- Paul, F., Kaab, A., Maisch, M., Kellenberger, T. & W. Haeberli, 2004: Rapid disintegration of Alpine glaciers observed with satellite data.- *Geophysical Research Letters*, 31, 21, article number L21402.
- Schaefli, B., Hingray, B. & A. Musy, 2007: Climate change and hydropower production in the Swiss Alps: quantification of potential impacts and related modelling uncertainties.- *Hydrology and Earth System Sciences*, 11, 3, 1191–1205.
- Seidel, K., Ehrler, C. & J. Martinec, 1998: Effects of climate change on water resources and runoff in an Alpine basin.- *Hydrological Processes*, 12, 10–11, 1659–1669.
- Senechal, G., Rousset, D., Salome, A.L. & J.R. Grasso, 2003: Georadar and seismic investigations over the Glacier de la Girose (French Alps).- *Near Surface Geophysics*, 1, 1, 5–12.
- Sharp, M., Gemmell, J.C. & J.L. Tison, 1989: Structure and stability of the former subglacial drainage system of the Glacier de Tsanfleuron, Switzerland.- *Earth Surface Processes and Landforms*, 14, 2, 119–134.
- Smart, C.C., 1983: The hydrology of the Castleguard Karst, Columbia Icefields, Alberta, Canada.- *Arctic and Alpine Research*, 15, 471–486.
- Smart, C.C., 1996: Statistical evaluation of glacier boreholes as indicators of basal drainage systems.- *Hydrological Processes*, 10, 4, 599–613.
- Smart, C.C., 1997: Hydrogeology of glacial and subglacial karst aquifers: Small River, British Columbia Canada.- In: P.Y. Jeannin (Ed.) *6<sup>th</sup> conference on Limestone Hydrology and Fissured Media*, 10–17 August 1997, La-Chaux-de-Fond, Switzerland. *Sciences et techniques de l'environnement*, 315–318, Besançon.
- Smart, C.C. & D.C. Ford, 1986: Structure and function of a conduit aquifer.- *Canadian Journal of Earth Sciences*, 23, 919–929.

Steck, A., Epard, J.L., Escher, A., Gouffon, Y. & H. Masson, 2001: *Carte tectonique des Alpes de Suisse occidentale et des régions avoisinantes 1:100000, Notice explicative.*- Service géologique national, Bern.

VAW, 2009: Swiss Glacier Monitoring Network.- [Online] <http://glaciology.ethz.ch/messnetz/index.html> [Accessed September 2009].

Viviroli, D. & R. Weingartner, 2004: The hydrological significance of mountains: from regional to global scale.- *Hydrology and Earth System Sciences*, 8, 6, 1016–1029.